Pergamon

Cement and Concrete Research 29 (1999) 1673–1680

CEMENT AND CONCRETE RESEARCH

# Behaviour of cement mortars containing an industrial waste from aluminium refining
# Stability in $Ca(OH)_2$ solutions

F. Puertas*, M.T. Blanco-Varela, T. Vazquez

*Instituto de Ciencias de la Construcción Eduardo Torroja (CSIC), P.O. Box 19002, 28033 Madrid, Spain*

Received 17 June 1998; accepted 14 July 1999

## Abstract

The physical and chemical interaction between a solid industrial waste from aluminium refining and saturated $Ca(OH)_2$ solution, as well as the effects of substituting siliceous sand for the waste on the physical and mechanical properties of mortars were studied. The waste is a solid that contains reactive alumina capable of combining with the calcium hydroxide. These reactions result in stable and insoluble compounds. This alumina, together with the halite (also present in the waste composition), chemically react with a saturated solution of $Ca(OH)_2$, giving as a main reaction product the so-called Friedel's salt ($Ca_4Al_2Cl_2O_6 \cdot 10H_2O$). Strätlingite and Si-hydrogarnets were among other products detected. The waste has a high specific surface area. The cement/waste mixtures therefore require a higher quantity of mixing water than cement/sand mixtures. The result is a decrease of the mechanical strengths and an increase of the total porosity. However, a decrease of the average size of the pores occurs, which can have a positive effect on the durability of the final material.

*Keywords:* Mortar; Mechanical properties; Waste management; $Ca(OH)_2$; Cement

## 1. Introduction

Recycling and reutilization of industrial waste and by-products are a subject of great importance today in cement and concrete technology. Traditional industrial by-products used in cement and concrete manufacture include fly ashes, granulated blast furnace slags, and silica fume. The reactivity and efficiency of these wastes as active additions (and even as cement constituents) have been extensively studied [1–3]. Less reactive wastes are used as load (charges) in the manufacture of cement or inert aggregates in the production of concretes and mortars.

Aluminium refining industries generate different solid wastes. One of them, called PAVAL™ has a high alumina content and can be used in applications such as raw material for cement manufacture (clay, bauxite, and kaolin substitutes), and refractory and ceramic materials, among others. Another application of this by-product is as an addition to the mortar as a partial substitute for the aggregates. This new mortar could be applied to make curbs, paving stones, pavements, and so forth.

The goals of this work are (1) to determine the chemical interaction between this waste (PAVAL™) and the Portlandite (the most reactive phase of Portland cement paste) and (2) to establish the effect on physicomechanical properties when silica sand is substituted for this waste in mortar.

## 2. Methods

### 2.1. Materials

The chemical analyses of the waste and the Portland cement used are shown in Table 1. The $SiO_2$ content in silica sand used as aggregate was 99% in mass. The mineralogy of the waste was characterized by X-ray diffraction (XRD), Fourier transform infrared spectroscopy (FTIR), scanning electronic microscopy with electron dispersive X-ray analysis (SEM/EDX), and transmission electronic microscopy with microanalysis (TEM). The cement used was characterized by XRD and FTIR.

A previous study [4] had proved that waste reactivity was related to the size of the particles, and that the maximum diameter of the particles was about 0.149 mm. The maximum diameter of the sand particles was set at 0.160 mm for the purpose of studying comparable materials. The particle size and surface area of PAVAL™ and silica sand

---

* Corresponding author. Tel.: +34-91-302-0440; fax: +34-91-302-0700.
*E-mail address*: puertasf@ietcc.csic.es (F. Puertas)

PII: S0008-8846(99)00157-X

Table1
Chemical analysis of the aluminium refining waste and cement II-F-35A

| Determinations (% mass) | Waste | Cement II-F-35A |
|---|---|---|
| Lost at 550°C | 9.70 | |
| Lost at 550–950°C | 2.15 | |
| Lost at 25–950°C | | 3.83 |
| Insoluble residue | | 0.85 |
| $Al_2O_3$ | 67.3 | 5.97 |
| $SiO_2$ | 4.14 | 17.63 |
| $Fe_2O_3$ | 1.00 | 2.59 |
| CaO | 4.83 | 63.76 |
| MgO | 6.03 | 0.95 |
| $SO_3$ | | 3.32 |
| $TiO_2$ | 0.69 | |
| MnO | 0.18 | |
| F | 3.7 | |
| Cl | 1.01 | |
| $Na_2O$ | 1.70 | 0.3 |
| $K_2O$ | 0.61 | 0.8 |
| Nitrogen amoniacal | 0.05 | |

were determined through laser granulometry and Brunauer, Emmett, and Teller (BET) method. The results obtained are presented in Table 2.

### 2.2. Tests

Two different studies were carried out in the present work. One test related to the chemical interaction between the waste and the Portlandite and a second test related to the physical and mechanical behaviour of mortars that contained the waste as a substitution of sand.

### 2.3. Waste $Ca(OH)_2$ interaction

The pozzolanic activity of the waste in accordance with Standard EN 196-5 [5] was evaluated to determine if there was a chemical interaction between the solid waste and $Ca(OH)_2$ solutions. Samples were analysed using XRD, FTIR, and SEM/EDX techniques at different ages (1, 3, 7, 15, and 28 days).

### 2.4. Physical and mechanical properties of waste Portland cement mortar

To determine the properties and physical and chemical characteristics of mortars when substituting waste for sand,

Table 2
Results from granulometry and BET methods carried out on sand and industrial waste

| | Laser granulometry | BET |
|---|---|---|
| Sand | ϕ <32 μm: 5.83% | 0.3254 ± 0.0068 $m^2/g$ |
| | ϕ <45 μm: 8.80% | |
| | ϕ <90 μm: 30.55% | |
| Waste | ϕ <32 μm: 55.26% | 19.1611 ± 0.1518 $m^2/g$ |
| | ϕ <45 μm: 63.39% | |
| | ϕ <90 μm: 71.95% | |

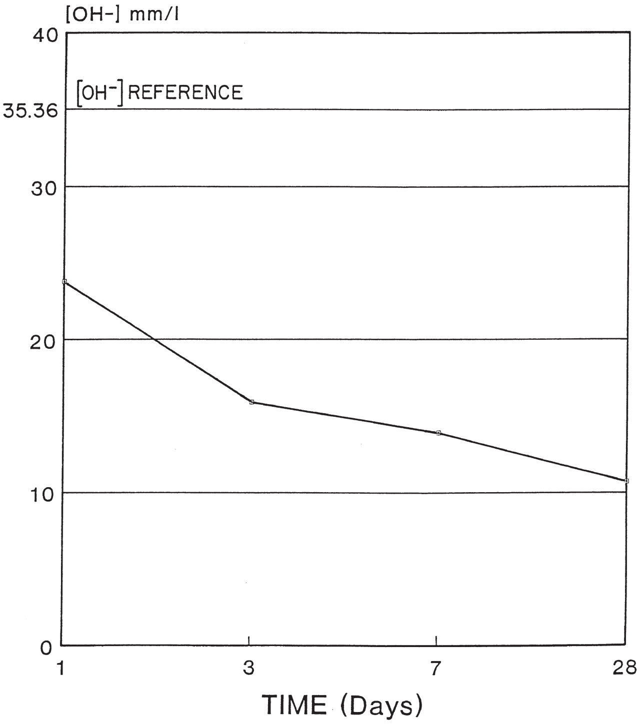

Fig. 1. Evolution of $OH^-$ in calcium hydroxide solutions in contact with the waste, as a function of time.

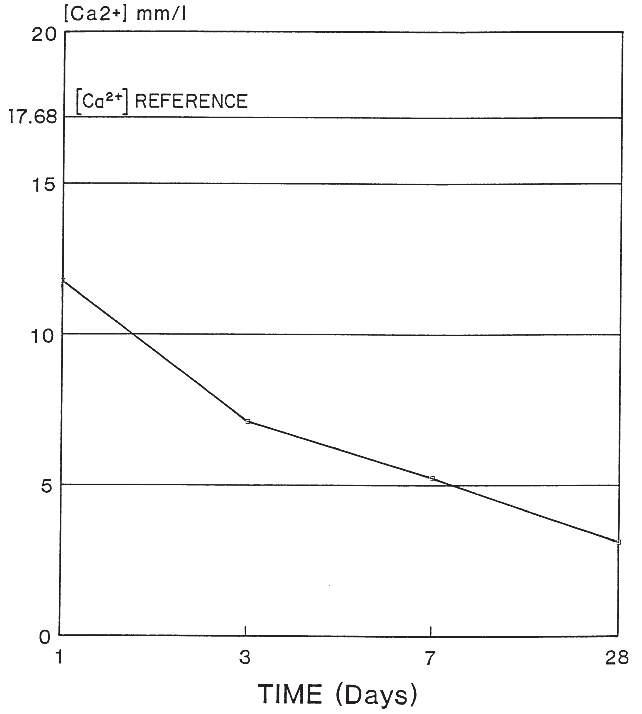

Fig. 2. Evolution of $Ca^{2+}$ in calcium hydroxide solutions in contact with the waste, as a function of time.

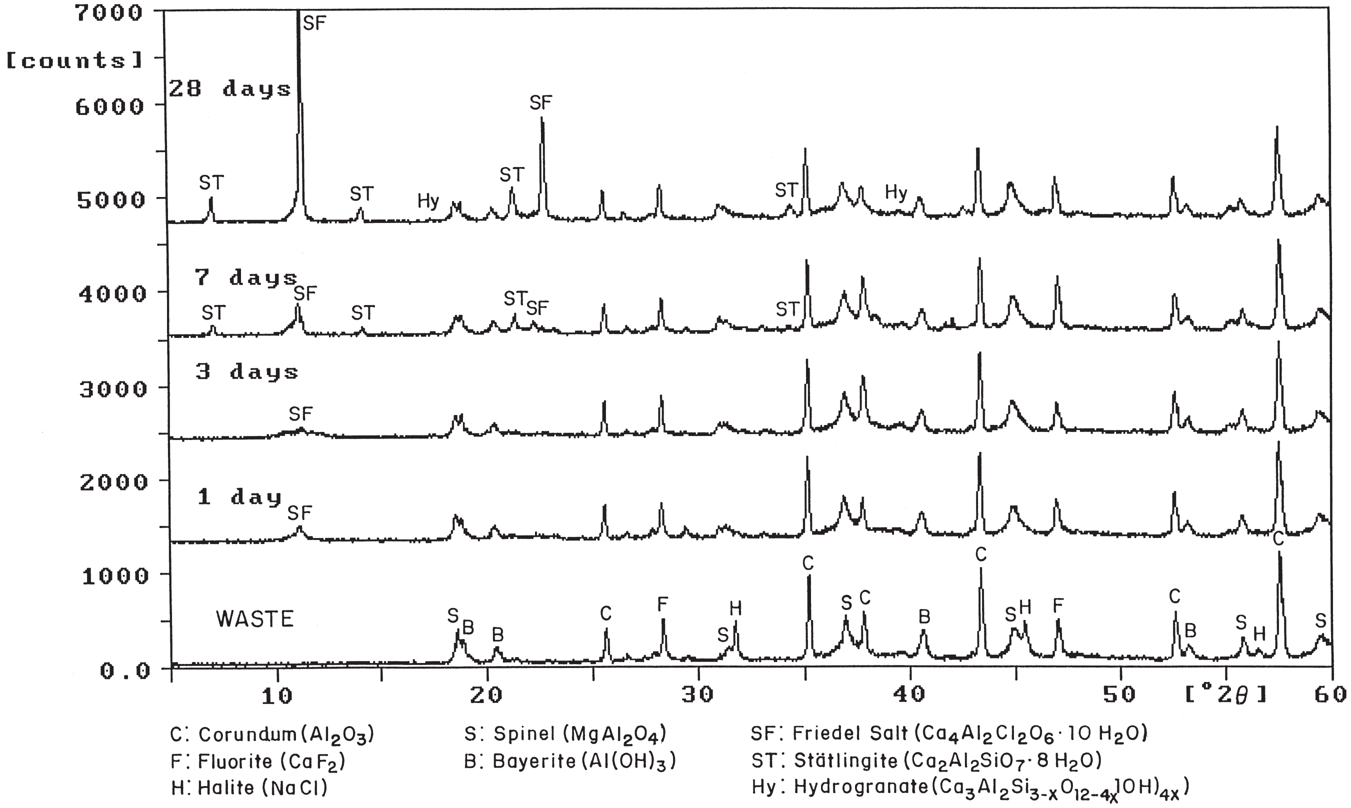

Fig. 3. Diffractograms of the wastes at the different ages of testing.

cement/waste mixtures were prepared with a mass ratio of 1/1.5, and cement/sand mixtures were prepared with an equal ratio. The following tests were carried out:

1. Determination of water/cement ratio for normal consistency of the mortar according to Standard UNE-102-96.
2. Setting time, according to Standard UNE-80.102-96.
3. Compression and flexural strengths at 3, 15, and 28 days. Prismatic samples of 1 × 1 × 6 cm were prepared according to Standard UNE-80.101.
4. Total porosity and pore size distribution through mercury intrusion porosimetry.

Finally, a calorimetric study on mixtures of cement/waste and cement/sand in equal proportion and of water/cement ratios equal to those used in the physicochemical tests was carried out. A J.A.F. conduction calorimeter (Wexham Developments, Berks, UK) was used and the final testing time was 45 hours.

## 3. Results

### 3.1. Mineralogical characterization of the waste

Results obtained using XRD and FTIR mineralogical characterization showed that the major compound of the waste is $Al_2O_3$ (corundum). The following minor compounds were also detected: spinel of the type $MgAl_2O_4$, $CaF_2$ (fluorine), NaCl (halite), and Al $(OH)_3$ (bayerite).

### 3.2. Interaction between solid waste and saturated solution of $Ca(OH)_2$

In Figs. 1 and 2 the evolution of $OH^-$ and $Ca^{2+}$ in calcium hydroxide solutions in contact with the waste as a function of time is represented. Both figures show that the concentrations $[OH^-]$ and $[Ca^{2+}]$ decrease as the contact time of the waste in the saturated solution increases. This fact indicates that $Ca(OH)_2$ is chemically combining with the product.

In Fig. 3, the X-ray diffractograms of the solid waste samples at the different ages of the test are represented. The diffractogram of the original product is represented as well. Analysis of the diffractograms show that the characteristic lines of the halite (NaCl) present in the waste disappeared at early contact with the calcium hydroxide saturated solution; also, the reflections from $Al(OH)_3$ (bayerite) were slightly affected.

After 1 day of interaction, Friedel's salt ($Ca_4Al_2Cl_2O_6 \cdot 10H_2O$) formed, as indicated by *d* spacings at 8.66 and 3.95 Å (Cu radiation). The intensity of these lines increased with interaction time, and after 28 days of reaction the peaks of Friedel's salt were the highest in the diffractogram.

At 7 days reaction the presence of some diffraction lines appeared at 12.50, 6.26, and 4.18 Å; these correspond to strätlingite ($Ca_2Al_2SiO_7 \cdot 8H_2O$). This compound is also known as "hydrated gehlenite." The amount of this phase increased after 28 days of interaction.

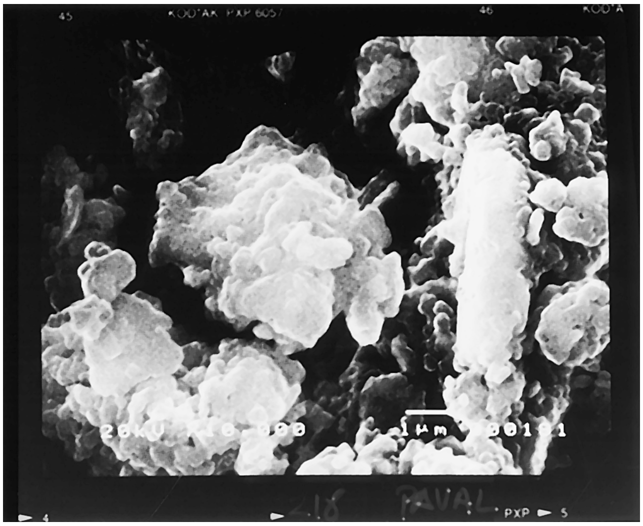

Fig. 4. PAVAL™ sample: large particle rich in Al.

After 3 days of interaction other lines of a very low intensity were observed at 5.08, 2.27, and 1.66 Å, which are probably due to the presence of a phase Si-hydrogarnet with a general formula: $Ca_3Al_2Si_{3-x}O_{12-x}(OH)_{4x}$ [6].

Results obtained through FTIR confirm the observations described above. There were some changes in the bands, assignable to the vibration of bayerite OH groups in the zone 3000–3700 cm$^{-}$1. This probably means that most of the aluminium, which had been combined during the treatment, came from an amorphous aluminium not detectable through XRD.

Microstructural analyses carried out on the original solid waste and on samples that had been in contact with $Ca(OH)_2$ solutions support the results already obtained through XRD. The original waste is a very heterogeneous material made up of agglomerated particles rich in aluminium (such is seen in Fig. 4). These particles made up the majority in the sample. Close to them are other needle-shaped particles with high contents of Si, Ca, and Al (whose chemical composition is close to that of gehlenite but they have not been identified through XRD). In Fig. 5 a micrograph of such particles is shown. The presence of halite (NaCl), fluorite, and spinel was also confirmed.

Fig. 5. PAVAL™ sample: needles with Al, Ca, and Si.

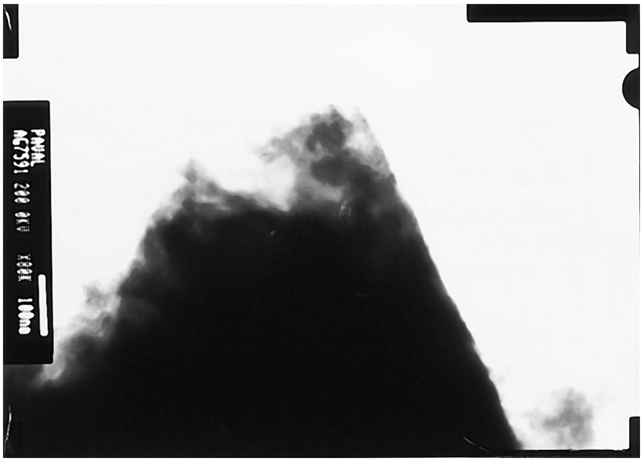

Fig. 6. PAVAL™ sample: TEM image, noncrystalline aluminum.

Analysis through TEM and electron diffraction revealed that the waste contains a noncrystalline aluminium-rich phase. This phase is found mainly in thicker particles, as seen in Fig. 6.

The morphology of the reaction products formed as a consequence of the interaction of the waste with the $Ca(OH)_2$ solution is presented in Figs. 7 and 8. Big crystals (over 20 μm) appearing in Fig. 7 have an elemental composition that corresponds to Friedel's Salt. Hexagonal plates of about 5–10 μm are identified according to their composition as strätlingite (Fig. 8).

### 3.3. Influence of the substitution of the sand for solid waste on the physical and mechanical properties of the mortars

From the results presented in Table 2 is inferred that although the maximum diameters of the sand particles and

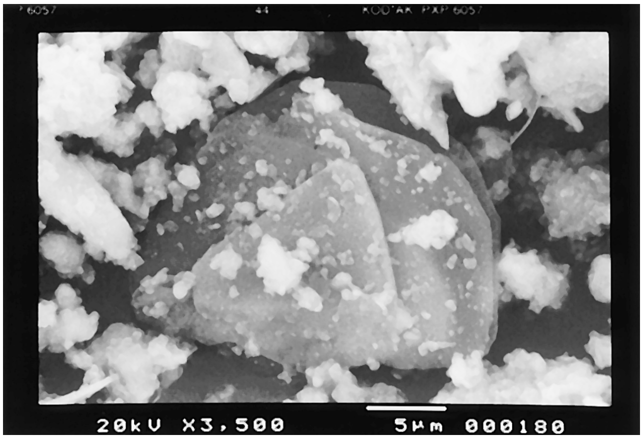

Fig. 7. Friedel salt particles. Sample of interaction between $Ca(OH)_2$ and PAVAL™ (28 days).

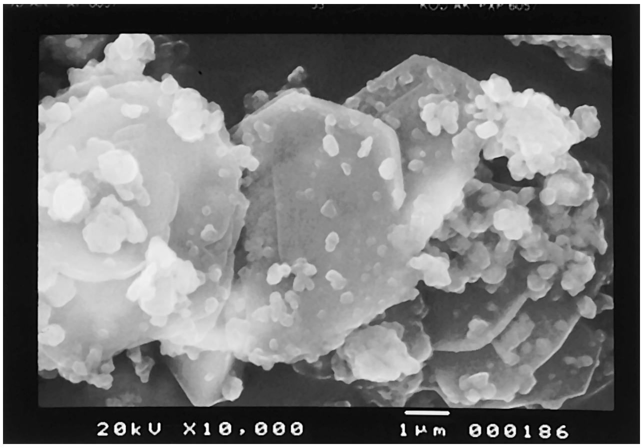

Fig. 8. Strätlingite particles. Sample of interaction between $Ca(OH)_2$ and PAVAL™ (28 days).

waste are basically the same, there are big differences in the particle size distributions and the surface areas of the materials. The amount of small size particles in the waste is much higher than in sand. Moreover, the surface area of the waste is 59 times larger than that of the sand.

Table 3 shows the results regarding the water requirements (water/cement ratio) for a normal consistency in mortars and values of initial and final setting times. The smaller size and the larger surface area of the waste particle size compared to those of the sand justifies the higher water requirements in cement/waste mixtures.

The results obtained after testing prismatic samples in compression and flexural tests are shown in Fig. 9. Mechanical strengths of cement/sand mixtures are, at all ages, higher than strengths developed by the cement/waste mixtures. This behaviour is more remarkable in flexural tests where the difference in strength values increases as the breaking age increases.

The total porosities of the mortars obtained through mercury intrusion porosimetry are shown in Table 4. Pore size distributions of these mortars are shown in Fig. 10. The total porosities of the cement/sand mixtures decrease slightly as the testing time increases, and they are always less than those in cement/waste mixtures. Total porosities of these mixtures remain constant for all the testing times. This behaviour is identical to the one observed in mechanical strengths.

The higher total porosities in mixtures containing PAVAL™, and their lower mechanical strengths are due to a higher water/cement ratio in the cement/waste mixtures vs. 0.73 to 0.54 for the cement/sand mixtures. However, the pore size distribution indicates that although the total porosities in the mortars with PAVAL™ are higher than in mortars with sand, the pore size is slightly smaller (Fig. 10).

Table 3
Water/cement ratio and setting times

| | | Setting times | |
|---|---|---|---|
| Mixture | Water/cement | Initial | Final |
| Cement/sand | 0.54 | 2 h 59 min | 3 h 24 min |
| Cement/waste | 0.73 | 4 h 54 min | 5 h 55 min |

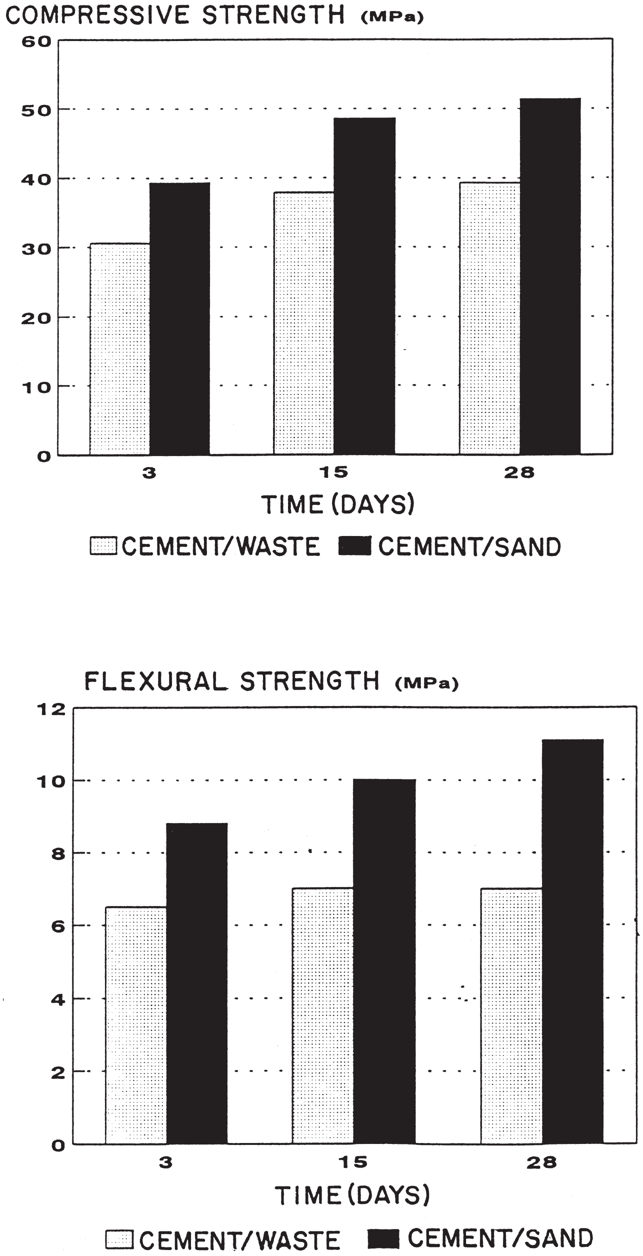

Fig. 9. Mechanical strength determinations for the standard cement-sand mortar and for the waste-substituted cement mortar.

### 3.4. Calorimetric studies

In the curves of heat evolution rate in cement/waste and cement/sand mixtures, the first peak of the curve cannot be seen clearly (Fig. 11a). This first peak is related to the heat released in the initial dissolution process of the anhydrous cement. After the induction period, the second peak appears, and it lasts longer and is more intense in cement/

Table 4
Total porosity

| Mixture and age of test | % Total porosity |
|---|---|
| Cement/sand | |
| 3 days | 18.72 |
| 15 days | 17.12 |
| 28 days | 16.46 |
| Cement/waste | |
| 3 days | 27.33 |
| 15 days | 27.99 |
| 28 days | 27.30 |

waste mixtures. Table 5 shows the values of intensity and time at which the maximum of the second peak of the curve of heat evolution rate appear. The maximum intensity in the heat evolution rate in the cement/waste mixtures indicates that join to chemical reactions that are taking place in the cement-water mixture, other reactions are involved due to the waste. This is confirmed by the higher heat release observed (Fig. 11b). However, the presence of PAVAL™ retards the cement hydration reactions.

## 4. Discussion

From the results of this study it is inferred that there is a chemical interaction between PAVAL™ and calcium hydroxide generated during the hydration of the clinker phases in Portland cement. Studies carried out through TEM on the solid waste revealed that it contains a significant amount of potentially reactive very low crystallinity alumina. As a consequence of the interaction of the waste with the $Ca(OH)_2$ saturated solution, the NaCl and a portion of this reactive alumina in the waste move toward the solution.

The conditions necessary to cause precipitation of Friedel's salt were reached quickly. It can be identified through XRD from the first reaction day. The amount of Friedel's salt in samples increased as the reaction time increased up to 28 days.

The waste contains 4.14% $SiO_2$, the composition of which is partly amorphous. No crystalline phase containing this oxide has been identified through XRD. It is a reactive $SiO_2$ since strätlingite is produced as a result of the chemical interaction between waste and calcium hydroxide solution. This compound was identified through XRD only after 7 days testing, and its content increased with reaction time.

Strätlingite formation was observed in studies of aluminous cement hydration in presence of blast furnace slags or other material carrying $SiO_2$ [7–12]. Different postulates try to explain the formation of this phase. In some cases formation of strätlingite is supposed to form through hexagonal aluminates (mainly $C_2AH_8$) and other cases through the cubic ($C_3AH_6$). The different origins are supported because the mechanical behaviour of the paste differs from one another. Accordingly, strengths would be higher in the case where strätlingite comes from hexagonal aluminate than from cubic phase.

No intermediate compounds have been observed that would justify strätlingite formation through the evolution of hydrated calcium aluminates either hexagonal or cubic. According to Damidot and Glasser [12], strätlingite can be in equilibrium with a series of Si-hydrogarnets, aluminium hydroxide, CSH gel, as well as with an aqueous solution of very similar composition. However, strätlingite is not stable

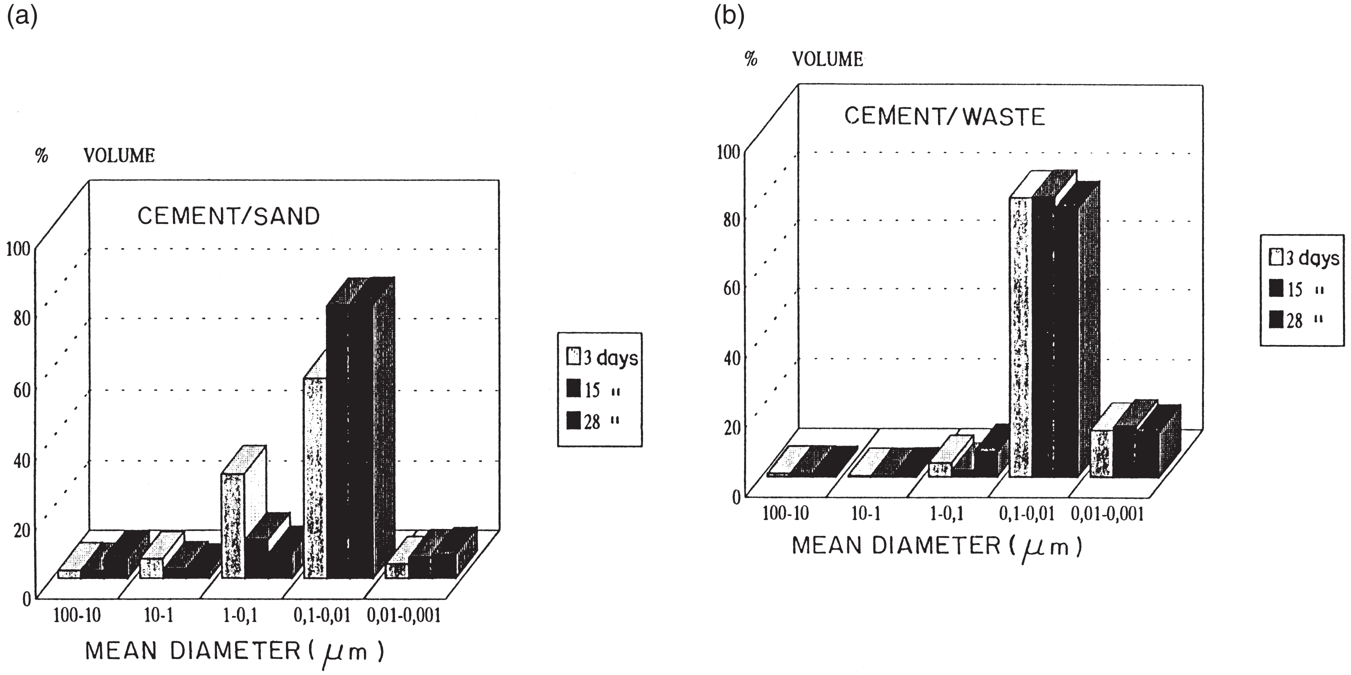

Fig. 10. Pore size distribution of the (a) standard mortar and waste-substituted mortar (b).

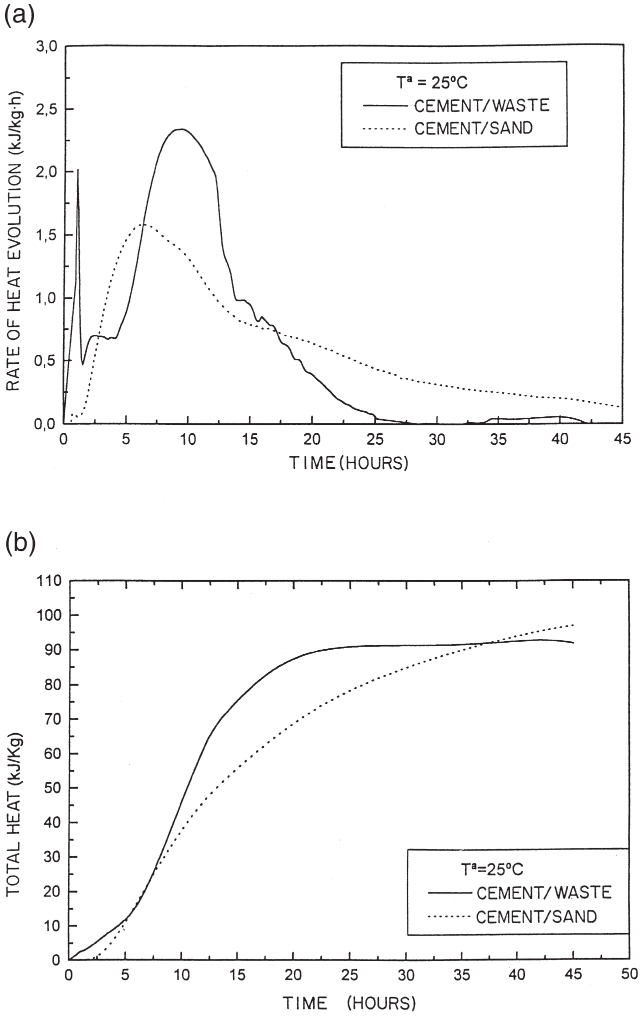

Fig. 11. Calorimetric data: (a) rate of heat evolution in function of time; (b) total heat in function of time.

in the presence of $Ca(OH)_2$, which would react to give hydrogarnets (in the absence of chloride ions). Given that the initial solution is saturated $Ca(OH)_2$, and even if alumina and silica would dissolve under these conditions, the required thermodynamic conditions for the precipitation of the strätlingite are not present. However, conditions for precipitation of the Friedel salt were reached in the first 24 hours of reaction. As a consequence of this precipitation, the concentration of $Ca^{2+}$ and $OH^-$ ions from the initial solution decreased, satisfying the required conditions for a joint precipitation of the strätlingite and the Friedel's salt. These conditions were reached after 7 days of reaction. Also, conditions for Si-hydrogarnet precipitation observed through XRD were reached.

The Friedel's salt is a reaction product that generally does not contribute to an increase in mechanical strength. Some authors [8,9] indicate the formation of strätlingite is associated with an increase of strength.

Physical characteristics of the PAVAL™ (high surface area and very small particles) explain its behaviour in cement mortar. Mixtures of cement/waste need a water content (for normal consistency) much higher than those required by cement/sand mixes. This accounts for the lower mechanical strengths (flexural and compression) and for the total porosity values. In addition, the high surface area of the waste makes it able to absorb a rather large amount of liquid. The presence of Cl and Na ions in the liquid modifies the activity of solution, decreasing the hydration rate of the main clinker phases.

Table 5
Heat evolution rate of the second peak and time when peak appears

| Mixture | $V_2$(Kj/Kg · h) | Time (hours) | Maximum heat (Kj/Kg) |
|---|---|---|---|
| Cement/sand | 1.58 | 6.20 | 91.74 |
| Cement/waste | 2.34 | 9.40 | 96.92 |

Nevertheless, in mortars with waste (although having higher porosity) the pore size distribution is characterized by having a higher proportion of small pores than the mixes without waste. The maximum sizes of the waste and sand particles are similar. The smaller pore diameters in the waste samples are due to the chemical interaction that occurs between the waste and cement and the surface characteristics of the waste itself. This small size of the average pore size in mixes with waste can affect the mortar permeability and consequently its chemical durability. More studies will be carried out to determine this influence.

## 5. Conclusions

The main conclusions drawn from this work are:

1. PAVAL™ contains reactive alumina that can combine with calcium hydroxide and form stable and insoluble compounds. This alumina, together with halite, chemically reacts in a $Ca(OH)_2$-saturated solution, giving as main reaction product the Friedel's salt ($Ca_4Al_2Cl_2O_6 \cdot 10H_2O$). Other products, like strätlingite and Si-hydrogarnets, have also been detected.
2. Cement/aluminium-rich waste mixes require a higher water/cement ratio than cement/sand mixes. The result is that cement/waste mixes show a decrease of mechanical strengths and an increase of the total porosity. However, their average pore size decreases.
3. A calorimetric study revealed that the waste retards hydration reactions in cement. There is an extension of more than 2 hours for the initial and final setting time. The high surface area of the waste makes it able to absorb a rather large amount of liquid. The presence of Cl and Na ions in the liquid modifies the activity of the solution, decreasing the hydration rate of the main clinker phases.

Calorimetric curves of cement/waste mixtures show longer peak of heat evolution rate than those of cement/sand mixtures. In addition to the heat released from cement hydration reactions, there is another additional heat source from the interaction between waste and cement paste compounds.

## Acknowledgments

Authors express their gratitude to REMETAL S.A. for providing the financial support for this research, within the ATYCA Project, an initiative of the Spanish Department of Industry and Energy. At the same time they want to thank Ignacio Alfaro from REMETAL S.A. for his collaboration, and M. Isabel Rodriguez-Maribona from LABEIN for her valuable comments and suggestions.

## References

[1] RILEM Technical Reports, 73-SBC RILEM Committee, Final report, Siliceous by-products for use in concrete, Materials and Structures 21 (121) (1988) 69–80.

[2] P.K. Metha, Puzzolanic and cementitious by-products in concrete. Another look, in: Third Canmet/ACI Trondheim Conference, 1989, pp. 1–43.

[3] R. Sersale, Advances in Portland and blended cements, in: IX Intern. Congr. Quim, Cem., Vol I, 1992, pp. 262–302.

[4] BRITE-EURAM Consortium, Report PR18, version 1.0, BRITE-EURAM Proyect, June 1997.

[5] EN 196-5, Métodos de ensayos de cementos: ensayo de puzolanicidad para cementos puzolánicos, 1998.

[6] T.G. Jappy, F.P. Glasser, Synthesis and stability of silica-substituted hydrogarnet $Ca_3Al_2Si_{3-x}O_{12-4x}(OH)_{4x}$, Adv Cem Res 4 (1) (1991/1992) 1–8.

[7] A.J. Majumdar, R.N. Edmonds, B. Singh, Hydration of calcium aluminate in presence of granulated blastfurnace slag, in: R.J. Mangabhai (Ed.), Calcium Aluminate Cements, E. and F.N. Spon, Cambridge, 1990, pp. 259–271.

[8] C.H. Fentiman, S. Rashid, J.P. Bayoux, A. Bonin, M. Testud, The effect of curing conditions on the hydration and strength development in fondu:slag, in: R.J. Mangabhai (Ed.), Calcium Aluminate Cements, E. and F.N. Spon, Cambridge, 1990, pp. 272–281.

[9] S. Bentsen, A. Seltveit, B. Sanberd, Effect of microsilica on conversion of high alumina cement, in: R.J. Mangabhai, E. and F.N. Spon, Cambridge, Calcium Aluminate Cements, 1990, pp. 294–303.

[10] Y. Ding, Y. Fu, Y. Beaudoin, Strätlingite formation in high alumina cement-silica fume system: Significance of sodium ions, Cem Concr Res 25 (6) (1995) 1311–1319.

[11] M.L. Romero, M.T. Blanco-Varela, A. Palomo, F. Puertas, T. Vazquez, Activation of blast furnace slag/high alumina cement pastes: Mechanical and microstructural evolution, in: X Intern. Congr. Chem. Cem. Gotenburg, Sweden, Vol. 3, 1997, pp. 3iii096 (8).

[12] D. Damidot, F.P. Glasser, Investigation of the $CaO$-$Al_2O_3$-$SiO_2$-$H_2O$ system at 25°C by thermodynamic calculations, Cem Concr Res 25 (1) (1995) 22–28.